Near-Ambient XPS Characterization of Interfacial Copper Species in Ceria-Supported Copper Catalysts

Manuel Monte[1,⊥,*], Guillermo Munuera[2], Dominique Costa,[3] José C. Conesa[1,*], Arturo Martínez-Arias[1,*]

[1] *Instituto de Catálisis y Petroleoquímica, CSIC, Marie Curie 2, 28049 Madrid, Spain.*
[2] *Departamento de Química Inorgánica, Universidad de Sevilla, 41092 Spain.*
[3] *Institut de Recherches Chimie-Paris, Physico-Chimie des Surfaces, UMR 8247 ENSCP ChimieParistech, 11 rue P. et M. Curie, 75005 Paris, France..*

Supporting Information

Structural/morphological characterization of the Catalysts. Main structural characteristics of the samples, on the basis of XRD, HRTEM, Raman spectroscopy and S_{BET} measurement, are summarized in Table S1 displayed below. Consideration of such results along with additional examination by XPS, H_2-TPR and EPR allowed to establish a structural model of the two examined catalysts (see main text).

Table S1. Specific surface area values, structural details extracted from analysis of the X-ray diffractograms and relevant parameters of the main fluorite F_{2g} Raman mode for the copper/ceria samples and corresponding ceria supports. CeO_2 crystallite size and microstrain values are based on analysis of the XRD peaks by means of Williamson-Hall linear fittings. Taken from ref. 1, in which full characterization details can be found.

Sample	CeO_2 crystallite size (nm)	CeO_2 lattice parameter a (Å)	Microstrain (Δd/d)	F_{2g} frequency (cm^{-1})	F_{2g} FWHM (cm^{-1})	S_{BET} (m^2g^{-1})
CeO_2-NC	46	5.406	0.00012	463	15.5	20
CeO_2-NS	7	5.410	0.0019	462	23.3	130
Cu/CeO_2-NC	42	5.404	0.00020	463	15.5	14
Cu/CeO_2-NS	7	5.410	0.0025	460	28.2	115

XPS characterization of the catalysts in their initial state. The two catalysts were examined in a laboratory apparatus (details elsewhere)[1] after subjecting them extendedly to ultrahigh vacuum at room temperature followed by static interaction with O_2/Ar (1/4 ratio, 10 Torr total pressure) in the spectrometer pretreatment chamber at 200 ^oC for 1 h, cooling to room temperature in the same oxidising atmosphere and final outgassing at room temperature prior to analysis under required ultrahigh vacuum conditions. In agreement with XRD/Raman characterization presented above and detailed elsewhere,[1] the spectra in the Ce(3d) zone (not shown) were characteristic of fully oxidised Ce^{4+} state with only a residual amount of Ce^{3+} being detected in any case. For copper, the Cu(2p) region shows main Cu($2p_{3/2}$) signal at 934.3 and 934.4 eV for Cu/CeO_2-NS and –NC, respectively, along with relatively intense satellite signals around ca. 942.5 eV, Figure S1, suggesting a predominance of Cu^{2+} state in any case. Joint consideration of such binding energy values along with Cu($L_3M_{45}M_{45}$) kinetic energy maxima at 916.3 and 916.2 eV, respectively (Figure S1), within a Wagner plot

⊥ Present address: European Synchrotron Radiat Facil**ity**, F-38043 Grenoble, France.

(Figure S2), confirms a basically fully oxidised state of copper in the initial catalysts subjected to oxidising pretreatment.

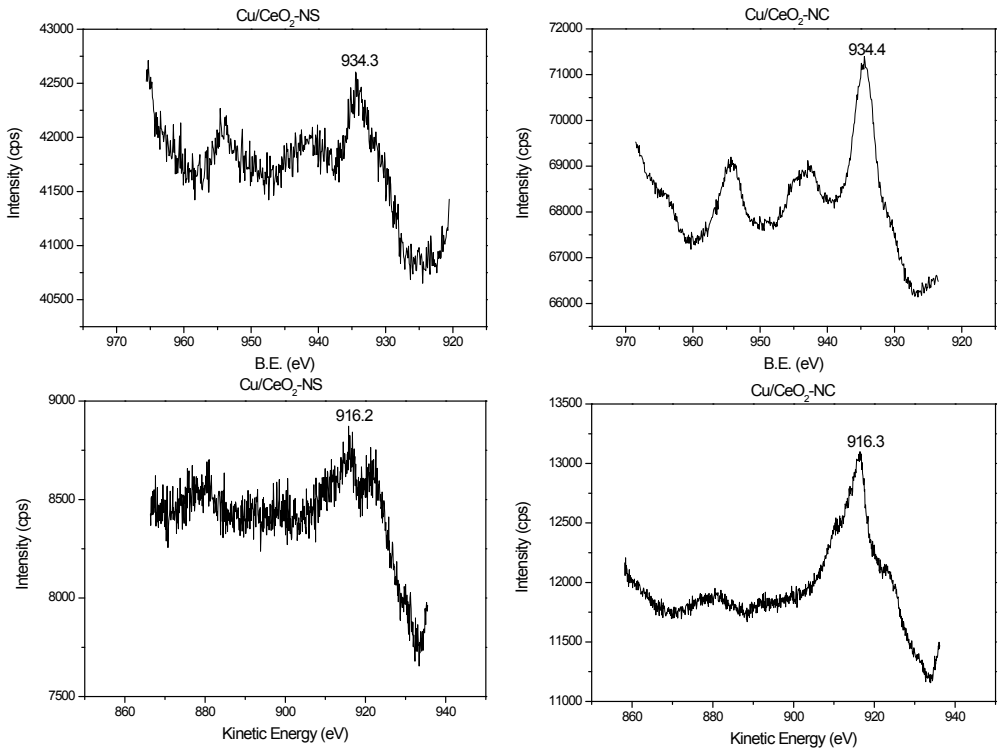

Figure S1. Cu(2p) XPS (top) and Cu($L_3M_{45}M_{45}$) Auger spectra (bottom) for the indicated samples after oxidising pretreatment. See main text for details on respective intensity. The signal at *ca.* 923 eV in the Auger spectrum of Cu/CeO_2-NS must be ascribed to the $NaKL_1L_1$ peak due to the presence of a small Na impurity in this sample, as detected in corresponding wide scan XPS spectrum.

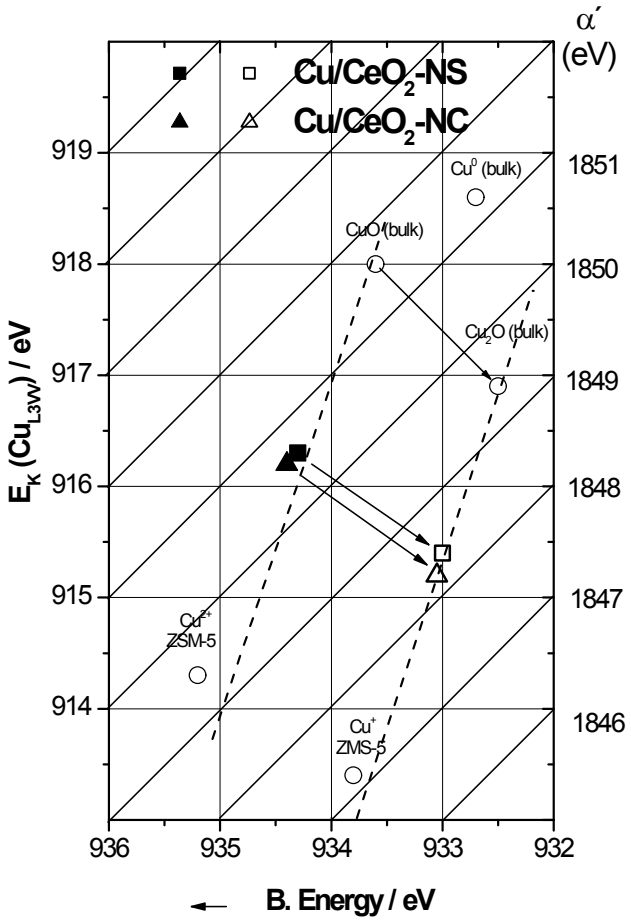

Figure S2. Wagner diagram (including lines with slope = −1 which correspond to constant values of Auger parameter labelled at the right side) showing the position of Cu (2p and AES) XPS parameters for the two initial samples subjected to oxidizing pretreatment (full square and triangle). Dashed lines with slope = -3 correspond to constant redox state of copper (e.g. CuO, Cu2O) according to Moretti's electrostatic model.[2] Open square and triangle close to the slope -3 line corresponding to the Cu+ state correspond to the samples after treatment under CO at 200 ^{o}C in the pretreatment chamber of the spectrometer, as shown elsewhere in detail.[1] Open circles correspond to the references employed to construct the diagram.

XPS results on regions Ce(3d), O(1s) and C(1s) for the samples reduced under CO. Ce 3d spectra for both samples and at all reduction temperatures examined appear quite similar to that of CeO_2-bulk nanoparticles,[3,4] as expected taking into account that ceria is the major component in both catalysts and its bulk reduction is not expected until relatively high reduction temperature is achieved.[1] For both samples, partial reduction of cerium is pointed out upon analysis of the spectra.[4,5] Thus, the spectra, representative examples being displayed in Figure S3, could be explained as the superposition of spectra from cerium (IV) and cerium (III), being the first one the main component in any case: for both samples the amount of Ce(III) is about 15 % at all examined temperatures. Both spin-orbit signals (5/2 and 3/2) of cerium (IV) are composed of three doublets (v´´´, v´´ and v, and u´´´, u´´ and u, respectively, using the typically used nomenclature for them)[6]. In turn, signals of cerium (III) are composed of two peaks spaced by 3-4 eV (simplified in the fitting of Fig. S3 as only one peak – u´ and v´ for 3/2 and 5/2 components, respectively -). The shift between spin-orbit doublets of 3d level is around 18 eV for both cerium (IV) and (III).

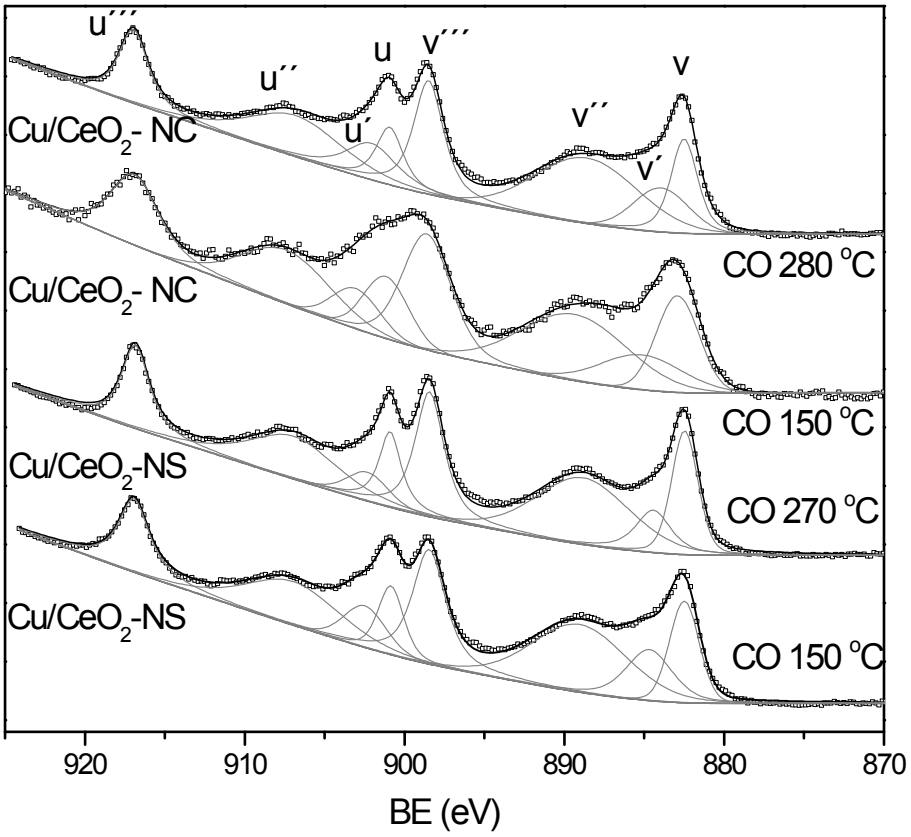

Figure S3. XPS spectra in the Ce(3d) region for the indicated samples reduced under diluted CO at the indicated temperatures. Fittings are only indicative, see text.

Concerning spectra in the O 1s region, they could be separated in at least three contributions at ca. 531.0, 529.7 and 529.0 eV, Figure S4. The first peak can be due either to carbonate or hydroxyl species known to be present in this type of samples under conditions similar to the ones here examined,[7] or to oxygens close to vacancies in correlation with proposed presence of a small amount of Ce^{3+}.[4] Note that, due to the basic character of ceria, the elimination of residual carbonates or hydroxyls through thermal decomposition under air typically requires relatively high temperature (above ca. 600 ºC) under which ceria sintering can take place. In turn, the peaks at ca. 529.0 and 529.7 eV can correspond to oxygens from different component oxides taking into account small differences between CeO_2/Ce_2O_3 (BE between 529.0 and 530.3 eV according to NIST-XPS database)[8] and CuO/Cu_2O (BE between 529.4 and 530.8 eV)[8]. Another possibility could be that they correspond to lattice and superficial oxygen in cerium oxide, respectively. This would be based on theoretical evaluation of core levels, which gives deeper values for bulk atoms (higher binding energy). Thus, differences of 0.5 and 0.7 are found between surface and bulk oxygen atoms in (111) and (001) models, which can explain the somewhat higher separation of those signals in Cu/CeO_2-NC. Note also in this sense that due to the relatively low amount of copper in the catalysts and even if considering its location at the surface of the samples, peaks due to

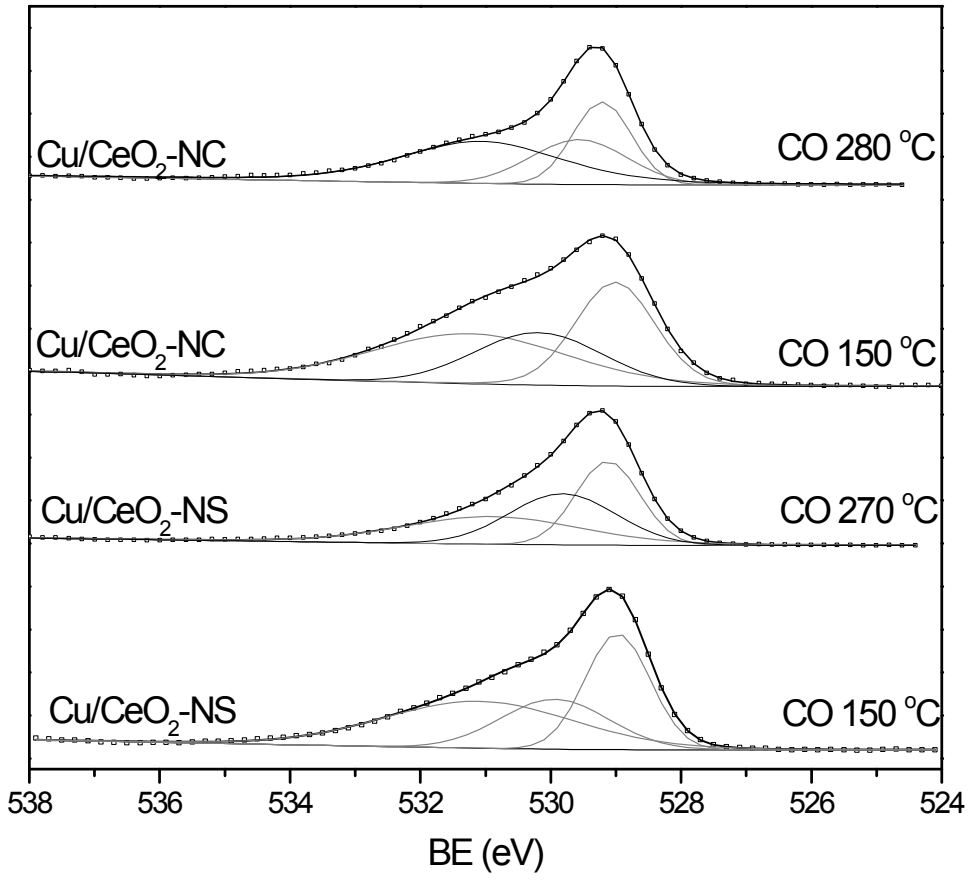

Figure S4. XPS spectra in the O(1s) region for the indicated samples reduced under diluted CO at the indicated temperatures.

oxygens from copper oxide appear could appear obscured since the observed spectra appear similar to those detected for the copper-free supports using a conventional laboratory equipment (not shown).

In turn, the C(1s) region is very similar for both samples at all examined temperatures and appears constituted by basically three signals, Figure S5. A first wide one centered at 292-293 eV is attributed mainly to gas phase CO; its wide shape suggests the overlapping with other contributions like CO_2(g), a satellite peak resulting from $\pi \rightarrow \pi^*$ transitions of graphitic carbon (see below) or carbonyls coordinated to cerium cations (probably occluded in subsurface regions, taking into account the bond would be relatively weak) known to be formed under CO at these relatively high temperature over this type of catalysts.[7] The second one at 288-289 eV is due basically to the Ce 4s photoelectrons although carbonate species, known to be formed upon interaction of these catalysts with CO,[7] can also appear overlapped in this position. The most intense contribution appears around 284-285 eV and is constituted by two signals. It can be due to carbonyl species,[9] although elemental carbon (graphitic- or diamond-like form, i.e. C_{sp^2}/ C_{sp^3}) also appears at this binding energy. The fact that its intensity does not decrease with increasing the temperature discards carbonyl species as main responsible for these signals, taking into account the thermal stability of such carbonyl species.[7] This is also corroborated by an independent experiment in which CO is removed from the flowing gas which apparently leads only to the elimination of the CO(g) contribution (Figure S6). Since carbonyls are expected to be removed under such condition,[7] signals at 284-285 eV must be attributed to elemental carbon formed through the Boudouard reaction

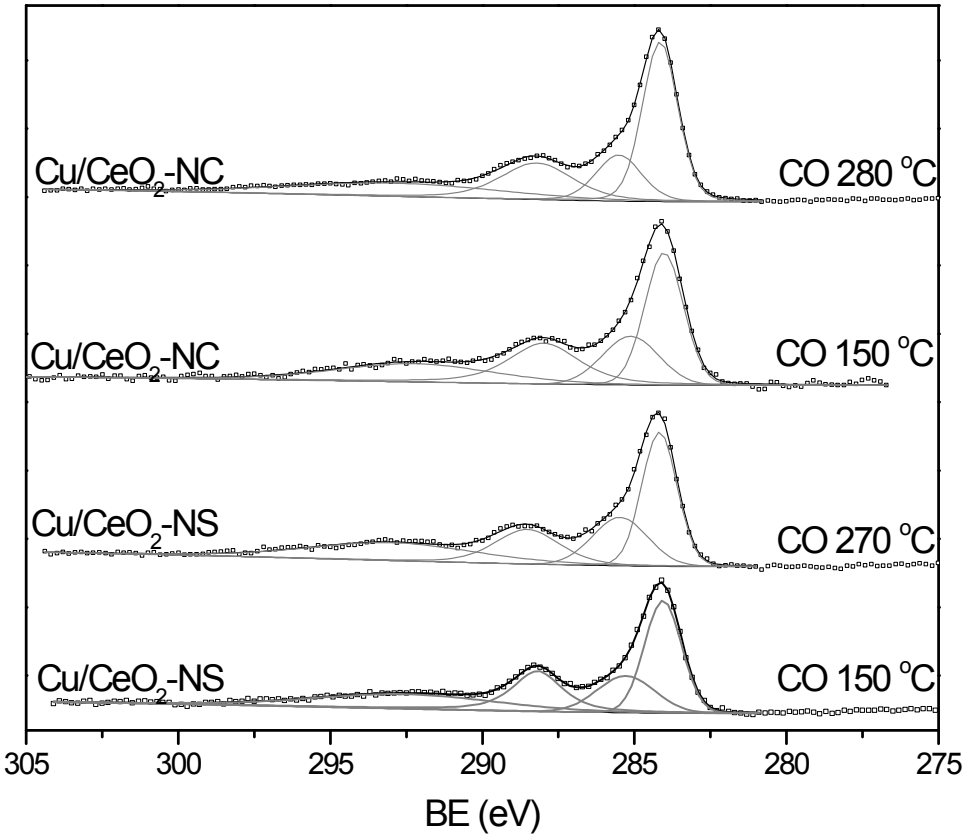

Figure S5. XPS spectra in the C(1s) (and Ce(4s), see text) region for the indicated samples reduced under diluted CO at the indicated temperatures.

(i.e. $2CO \rightarrow C + CO_2$) while copper-related carbonyls most likely provide a smaller contribution (considering the relatively small amount of copper employed) which becomes obscured by the stronger signal of elemental carbon. In any case, it must be noted that a certain coverage by carbon species contributing to signals at 284-285 eV is produced since C/(Cu+Ce) atomic ratios calculated (considering adequate electron inelastic mean free paths for the employed energies and materials and photoionization cross-sections under experimental conditions employed and for corresponding orbitals)[10, 11] were of ca. 0.11 and 0.22 for Cu/CeO_2-NS and Cu/CeO_2-NC, respectively.

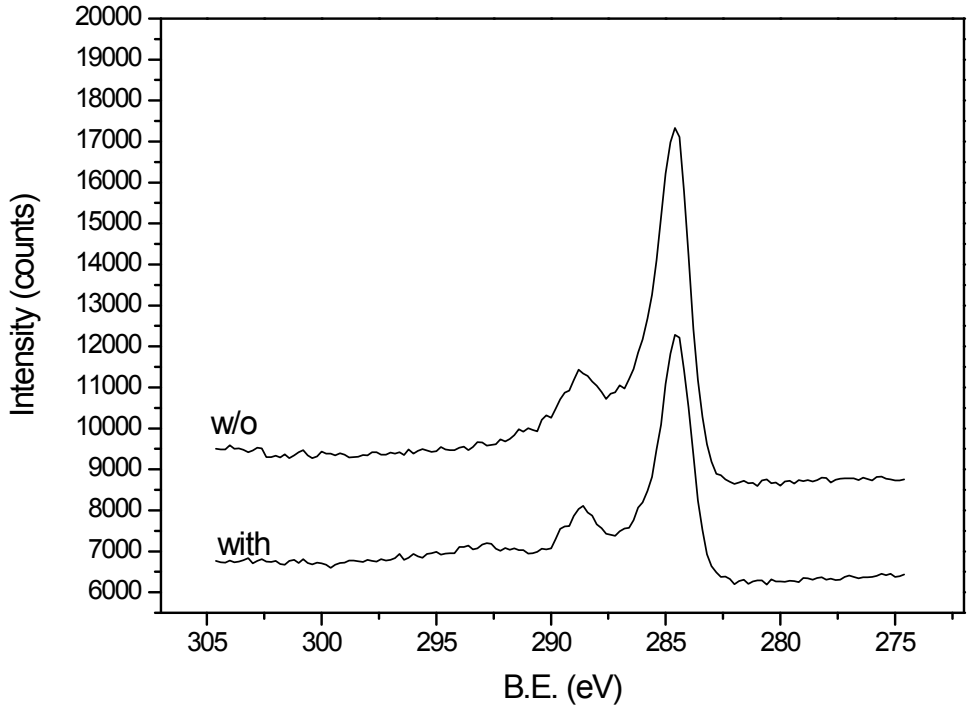

Figure S6. XPS spectra in the C(1s) region for Cu/CeO_2-NS at 180 ^oC in the presence/absence of CO in the flowing stream. Differences in respective intensity are related to the photoelectron screening effects of the gas around the sample in each case.

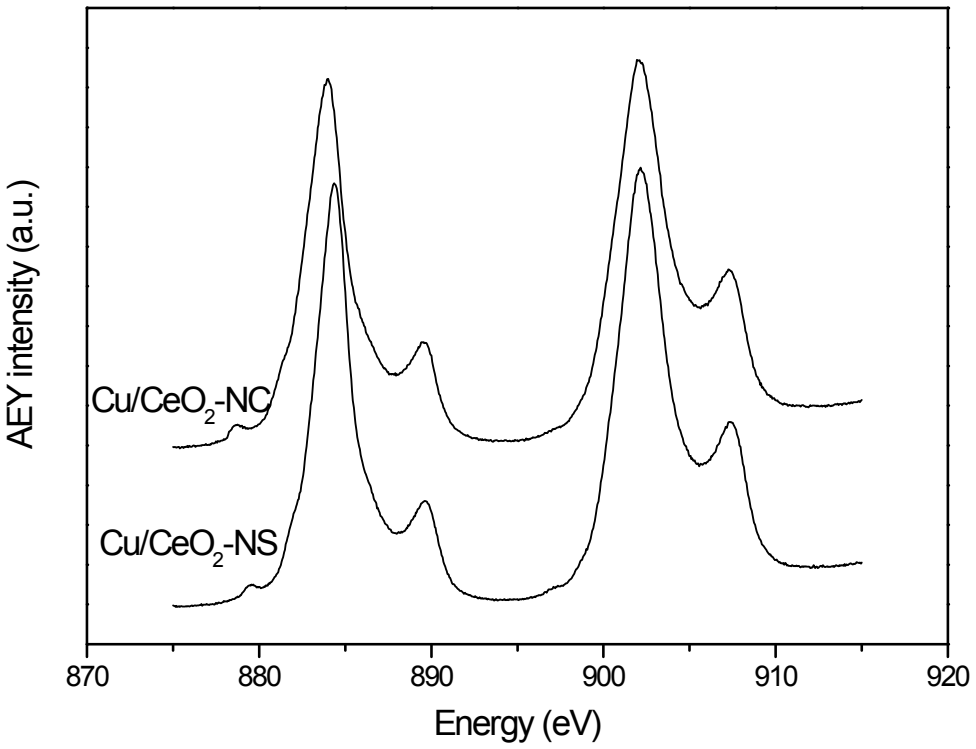

Figure S7. XANES spectra at the Ce M-edge for the indicated samples registered under diluted CO flow (5% in He at 100 Pa) at 150 ^{o}C. Spectra are similar to those detected for pure CeO_2 in the scientific literature with maxima at around 884.1 and 902.0 eV.[12]

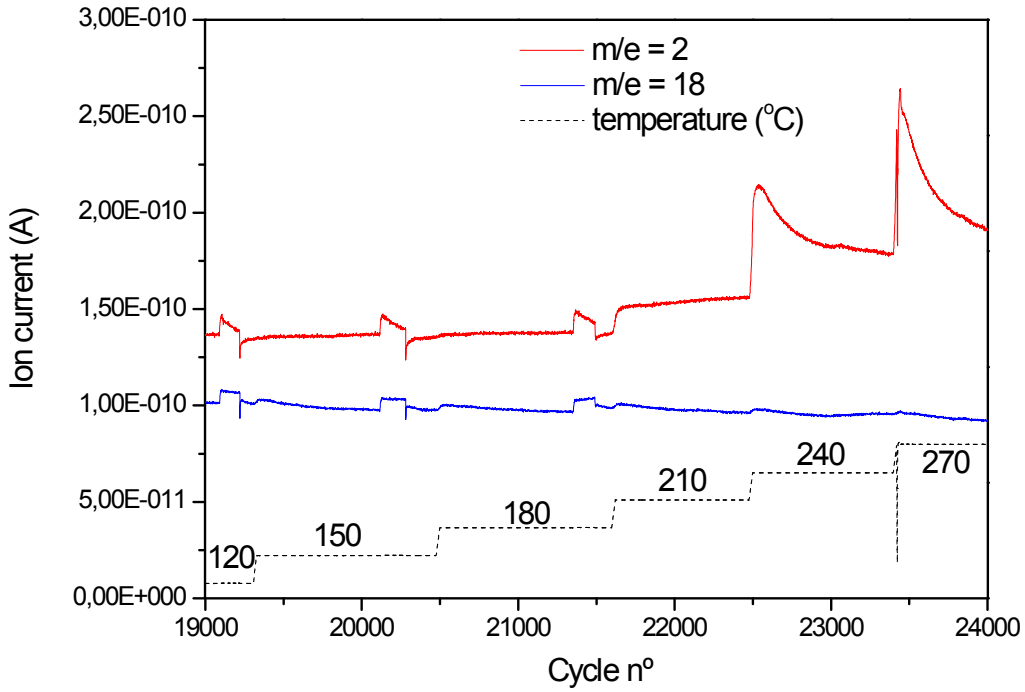

Figure S8. Evolution of H_2 (related to the m/e = 2 MS signal) during the course of the interaction of Cu/CeO_2-NS with diluted CO flow under stepwise increasing temperatures. The H_2 evolution (related to WGS activity) observed at the higher temperatures must originate from (the reaction of CO with) the surface hydroxyls since practically no change is detected in the water signal (related to m/e = 18) when H_2 appears above 210 ºC, in turn indicating the absence of residual water in the reactant flow.[13] The latter interpretation is also inferred from the shape of the m/e = 2 signal evolution under WGS reaction - above 210 ºC – which displays a maximum and a more or less rapid return to the baseline, thus basically reflecting that the reactant providing the hydrogen is present in a limited amount, as expected for surface hydroxyls present in the samples (according to analysis above).

Different models employed for the theoretical calculations. In order to study the core level shift in the models which represent the catalysts different references have been taken into account: an internal reference (figure S9.B) and a external reference (figure S9.C).

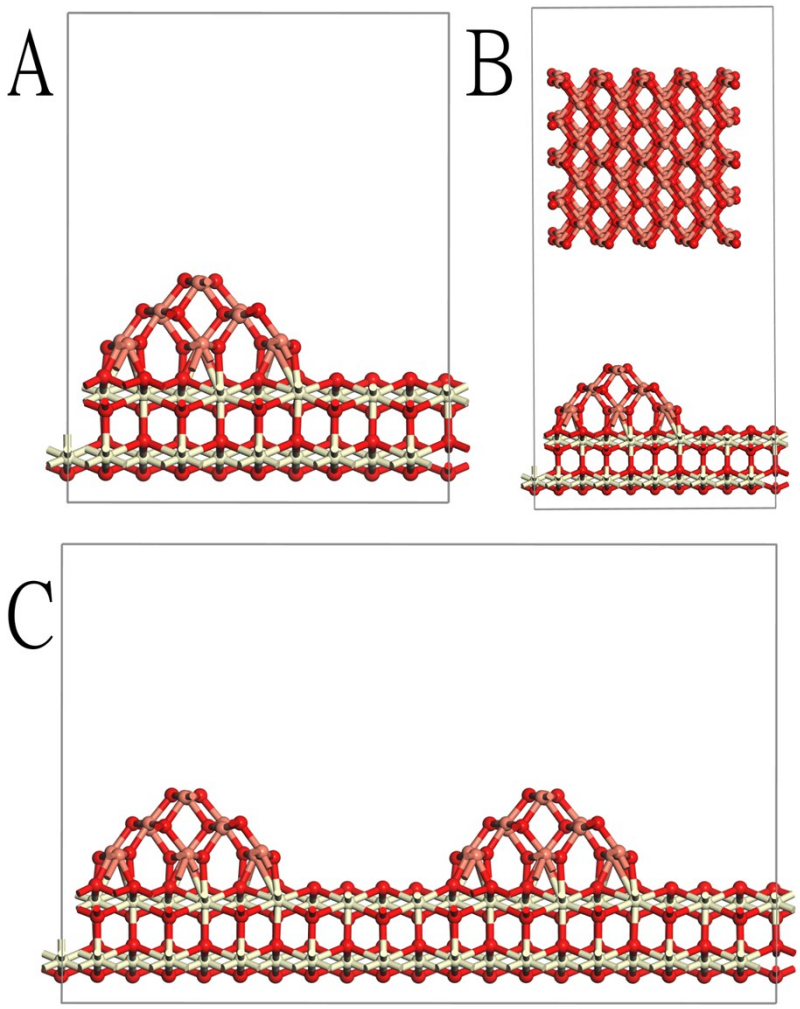

Figure S9. A (top left): normal model for geometry optimization. B (top right): model with a external reference. The cluster (CuO or metallic Cu) is used to obtain the basic CLS of the oxidised copper particle with respect to normal compounds of copper. C (bottom): double model with an internal reference for CLS calculation. This model allows having one copper particle fully oxidised and one copper particle partially (or totally) reduced most useful to compare the shifts in the core levels of copper atoms.

References

[1] D. Gamarra, A. López Cámara, M. Monte, S.B. Rasmussen, L.E. Chinchilla, A.B. Hungría, G. Munuera, N. Gyorffy, Z. Schay, V. Cortés Corberán, J.C. Conesa, A. Martínez-Arias. *Appl. Catal. B* 2013, **130-131**, 224-238.

[2] G. Moretti. *J. Elec. Spectr. Rel. Phenom*. 1998, **95**, 95-144.

[3] Y.A. Teterin, A.Y. Teterin, A.M. Lebedev, I.O. Utkin. *J. Elect. Spectr. Rel. Phenom.* 1998, **88-91**, 275-279

[4] J.P. Holgado, R. Alvarez, G. Munuera. *Appl. Surf. Sci.* **2000**, 161, 301-315.

[5] F. Le Normand, J. El Fallah, L. Hilaire, P.I. Légaré, A. Kotani, J.C. Parlebas. *Sol. St. Commun*. 1989, **71**, 885-889.

[6] R.M. Ferrizz, T. Egami, G.S. Wong, J.M. Vohs. *Surf. Sci.* 2001, **476**, 9-12

[7] P. Bera, A. López Cámara, A. Hornés, A. Martínez-Arias. *J. Phys. Chem. C* 2009, **113**, 10689-10695.

[8] NIST-XPS Database 20 version 4.1; http://srdata.nist.gov/XPS.

[9] V.V. Kaichev, I.P. Prosvirin, V.I. Bukhtiyarov, H. Unterhalt, G. Rupprechter, H.-J. Freund. *J. Phys. Chem. B* 2003, **107**, 3522-3527.

[12] S. O. Kucheyev, B.J. Clapsaddle, Y.M. Wang, T. van Buuren, A.V. Hamza. Phys. Rev. B 2007, **76**, 235420.

[10] NIST X-ray photoelectron spectroscopy database: http://srdata.nist.gov/xps/

[11] J.J. Yeh, I. Lindau. Atom. Dat. Nucl. Dat. Tabl. 1985, **32**, 1-155.

[12] S. O. Kucheyev, B.J. Clapsaddle, Y.M. Wang, T. van Buuren, A.V. Hamza. Phys. Rev. B 2007, **76**, 235420.

[13] Kj. Kundakovic, D.R. Mullins, S.H. Overbury *Surf. Sci.* 2000, **457**, 51-62